Variability of the Australian Monsoon and Precipitation Trends at Darwin

STUART EVANS, ROGER MARCHAND, AND THOMAS ACKERMAN

Department of Atmospheric Sciences, and Joint Institute for the Study of the Atmosphere and Ocean, University of Washington, Seattle, Washington

(Manuscript received 16 July 2013, in final form 16 July 2014)

ABSTRACT

An atmospheric classification for northwestern Australia is used to define periods of monsoon activity and investigate the interannual and intraseasonal variability of the Australian monsoon, as well as long-term precipitation trends at Darwin. The classification creates a time series of atmospheric states, which two correspond to the active monsoon and the monsoon break. Occurrence of these states is used to define onset, retreat, seasonal intensity, and individual active periods within seasons. The authors demonstrate the quality of their method by showing it consistently identifies extended periods of precipitation as part of the monsoon season and recreates well-known relationships between Australian monsoon onset, intensity, and ENSO. The authors also find that onset and seasonal intensity are significantly correlated with ENSO as early as July.

Previous studies have investigated the role of the Madden–Julian oscillation (MJO) during the monsoon by studying the frequency and duration of active periods, but these studies disagree on whether the MJO creates a characteristic period or duration. The authors use their metrics of monsoon activity and the Wheeler–Hendon MJO index to examine the timing of active periods relative to the phase of the MJO. It is shown that active periods preferentially begin during MJO phases 3 and 4, as the convective anomaly approaches Darwin, and end during phases 7 and 8, as the anomaly departs Darwin. Finally, the causes of the multidecadal positive precipitation trend at Darwin over the last few decades are investigated. It is found that an increase in the number of days classified as active, rather than changes in the daily rainfall rate during active monsoon periods, is responsible.

1. Introduction

Northern Australia experiences a strong monsoon cycle over the course of the year. During austral winter, dry continental air from the southeast makes rainfall both rare and weak. Beginning in September, a transition period gradually increases temperature and moisture in the region, leading to more clouds and precipitation. The monsoon is generally considered to begin at some point in December when the winds become steady westerlies, bringing large amounts of tropical moisture to northern Australia (Hung and Yanai 2004). The vast majority of northern Australia's rainfall comes during the monsoon wet season, continuing from December into March or April (McBride and Nicholls 1983). During this period, the monsoon occasionally undergoes break periods, during which winds are easterly and rainfall is less frequent (Holland 1986). As the major source of rainfall for the region, variability in the onset, retreat, and intensity of the monsoon is of substantial importance to northern Australia.

Predictability of various metrics of the Australian monsoon has been an active topic of research for decades. Onset date and its relationship to the El Niño–Southern Oscillation (ENSO) is a particularly well-studied feature of the monsoon. Many different definitions of monsoon onset have been created over the years. Nicholls et al. (1982) created precipitation-based definitions of monsoon onset, defining it as the date by which various cumulative precipitation totals have been reached at Darwin, Australia. Others, such as Holland (1986), Drosdowsky (1996), and Kajikawa et al. (2010), have used wind-based definitions to identify monsoon onset: for example, when the zonal winds, either at a particular level at Darwin (Holland 1986), vertically averaged (Drosdowsky 1996), or averaged across the region (Kajikawa et al. 2010), reverse direction and become westerly. Still others have created multivariate definitions to identify monsoon onset. Hendon and Liebmann (1990), for example, defined onset as the first

Corresponding author address: Stuart Evans, University of Washington, 408 ATG Building, Box 351640, Seattle, WA 98195-1640.
E-mail: sevans@atmos.washington.edu

DOI: 10.1175/JCLI-D-13-00422.1

simultaneous occurrence of westerly winds and widespread rainfall in northern Australia.

Regardless of the definition, it is universally agreed that there is a strong relationship between onset date and ENSO activity. Sea surface temperatures (SSTs) around northern Australia are affected by ENSO. During La Niña, SSTs are greater, leading to enhanced convection and precipitation (Catto et al. 2012b). As a result, La Niña conditions in the months leading up to onset (September–November) are usually associated with an earlier monsoon onset. La Niña conditions also tend to favor a more intense monsoon season, whether this is measured as total seasonal rainfall (e.g., McBride and Nicholls 1983), number of active days (Drosdowsky 1996), or strength of an index based on westerly wind speed in the region (Kajikawa et al. 2010). In contrast, the retreat date for the monsoon has not been found to be correlated with ENSO indices at any lead time (e.g., Drosdowsky 1996), and the causes of its variability are, to the best of our knowledge, unknown.

The Madden–Julian oscillation (MJO; Madden and Julian 1972) is the major source of variability in the tropics on intraseasonal time scales (Zhang 2005). Previous studies have focused on two characteristics of the Australian monsoon that may be affected by the MJO, onset date and the frequency of active periods. Hendon and Liebmann (1990) composited zonal winds and outgoing longwave radiation (OLR) at various leads and lags of their onset date to show that the monsoon begins with the passage of an MJO event that begins in the Indian Ocean. An analysis of the frequency of active periods is limited to those studies and techniques that define individual active periods within a season, not just an onset date. Of those who do define active periods, Holland (1986) found that the mean period from the start of one active period to the next is 40 days, implying that the MJO plays a role in the timing and duration of active periods; however, Drosdowsky (1996) challenged this, showing that there is no preferred duration or interval time for active periods under his definition, and speculated that the low-pass filtering of winds in the Holland study contributed to the apparent presence of a 40-day period. Both of these studies predate the very useful definition of MJO phases by Wheeler and Hendon (2004), which provides a new way of analyzing the timing of active periods, complementing previous methods that used spectral analysis to detect the influence of the MJO. To the best of our knowledge, the role of the MJO in regulating active periods of the monsoon remains an unresolved question, and an analysis of the timing of individual active and break periods relative to the phase of the MJO has not been undertaken.

Observations suggest that over recent decades precipitation has increased in northern Australia. Hennessey et al. (1999) found a significant increase in the number of days with rain over the twentieth century, while Taschetto and England (2009) found that the positive trend in northern Australia precipitation from 1970 to 2006 is primarily due to an increase in the number of deep convection rainfall events. Whether these trends are as result of changes in the frequency of occurrence of various circulation patterns or changes in the number of deep convection events associated with particular circulation patterns is an interesting question. Catto et al. (2012a) use a regime classification to address this question and conclude that an increase in the frequency of occurrence of monsoon regimes was responsible for the trend from 1957 to 2007. Evans et al. (2012) also define a classification for the northern Australia region that can be used for this purpose and could provide additional insight into whether it is changes in the frequency of circulation patterns or the precipitation associated with them that is responsible.

In this study, we make use of an atmospheric classification described in Evans et al. (2012) to examine the relationships between the MJO and the timing of active and break periods of the Australian monsoon, as well as to further investigate the contributors to the long-term trend in precipitation at Darwin. The classification produced definitions of eight atmospheric states for a region centered on Darwin, of which states 7 and 8 will be the focus of this study, as they represent conditions during the active monsoon and break monsoon, respectively. We choose this technique because its objective classes allow for both the identification of individual active periods for the MJO analysis and the decomposition of the precipitation trend into contributions from a variety of classes. We also use the well-established relationships between the monsoon and ENSO as a test of the classification's ability to identify monsoon periods. In section 2, we describe the process of defining the atmospheric states, describe our identification of states 7 and 8 as the active and break monsoon, and define metrics for various characteristics of the monsoon season (e.g., onset date). In section 3, we demonstrate the validity of our atmospheric classification metrics by showing that they consistently place most of the precipitating periods within the monsoon season and capture the previously identified relationships between the onset and monsoon season intensity of the Australian monsoon and ENSO. Sections 4 and 5 present new results pertinent to understanding how the MJO affects the timing of both active and break periods of the monsoon and long-term trends in the occurrence of monsoon conditions and precipitation at Darwin, respectively. Further analysis and potential future work are discussed in section 6.

2. Characterizing the monsoon

We determine the timing of monsoon events using a set of atmospheric states for the northern Australia region previously created and described in Evans et al. (2012; hereafter E12). The process of defining the states and the states themselves are described in detail in E12; we summarize the salient details here. The states are defined by a cluster analysis algorithm first developed by Marchand et al. (2009) that uses reanalysis products as the inputs. E12 uses European Centre for Medium-Range Weather Forecasts (ECMWF) Interim Re-Analysis (ERA-Interim) temperatures, horizontal winds, relative humidity values, and surface pressure values sampled on a grid spanning 121°–141°E and 4.5°–20.5°S and at seven vertical levels from the surface to 250 hPa. Collectively, these five variables on the three-dimensional grid compose a single snapshot in time of the atmosphere for a region surrounding Darwin, Australia. Approximately four years of snapshots taken every six hours were input to the clustering algorithm. An issue common to all clustering studies is determining the correct number of clusters. E12 uses independent observations of the vertical distribution of cloud occurrence, as observed by the millimeter cloud radar at the Darwin Atmospheric Radiation Measurement Program (ARM) site, to test the clusters for statistical significance. Two tests are applied: whether the observed vertical profile of cloud occurrence for each cluster is stable in time and whether the cloud occurrence profiles for each cluster are distinct from each other. E12 tests stability by comparing the cloud profiles from the first half of the dataset to those of the second half. States with profiles that are statistically similar in both halves of the dataset are considered stable. Similarly, states with profiles that are statistically different from the profiles of all the other states are considered distinct. Clusters with associated cloud profiles that do not pass one of these tests are deemed to be poorly defined, and their member snapshots are resorted into the other clusters. An iterative process refines both the number of clusters and their definitions in order to ensure that all clusters have, in a statistical sense, cloud occurrence distributions that are both temporally stable and distinct. The final product is a set of eight clusters representing the most frequently occurring weather patterns within the Darwin region. Each cluster is called an atmospheric state, and we define it by the mean of its member snapshots.

Occurrence of the eight atmospheric states has a strong seasonal signal. States 1–4 are all dry season states, occurring almost exclusively between April and September. States 5 and 6 are transition season states and occur primarily from March to May and from September to November. Here we focus on states 7 and 8, which occur primarily during the monsoon season from December to April. E12 identified state 7 as the active monsoon and state 8 as the monsoon break based on their composite meteorology, cloud occurrence profiles, and rain rates. Selected fields of the composite meteorology of states 7 and 8 are shown in Fig. 1 along with vertical profiles of cloud occurrence and distributions of rain rate. State 7, the active monsoon, has deep westerly winds with cyclonic rotation and moist northwesterly surface flow near Darwin, low surface pressure (not shown), and high relative humidity throughout the troposphere. It is the cloudiest and rainiest of the states, as befitting a state with moist flow from the tropics and large-scale ascent. State 8, the break monsoon, has easterly flow at the surface near Darwin becoming southeasterly and anticyclonic with height. While still humid, cloudy, and rainy compared to the dry and transition season states, it is less so than the active monsoon.

Because our state definitions are based on ERA-Interim data, we are able subsequently to classify every time step of the Interim period into one of the eight states by calculating the Pythagorean distance from each reanalysis snapshot to each of the eight state definitions. The snapshot is then classified as the state to which it is closest. In doing so, we create a 34-yr time series from 1979 to 2012 of atmospheric state for the region surrounding Darwin (containing 33 complete monsoon seasons). This time series allows us to create simple metrics describing the Australian monsoon. We define the onset of the monsoon as the first time each season four consecutive snapshots (24 h) are classified as the active monsoon. Similarly, monsoon retreat is the last time each season that there are 24 continuous hours of active monsoon. During the monsoon season, the beginning and end of individual active periods are identified the same way. We describe the intensity of the monsoon by two metrics: the number of active days each year and the fraction of all monsoon days each year (states 7 and 8) that are classified as active (state 7).

As an example, the top panel of Fig. 2 shows the time series of atmospheric state for the 1981/82 season, with the onset, retreat, and active periods as defined by the metrics above. The atmospheric state begins the year varying among the dry season states, spends much of September and October in the transitional states, and then nearly exclusively inhabits one of the two monsoon season states from onset in late November until April. The bottom panel shows the daily precipitation for the season, demonstrating how it increases in frequency and intensity during active periods of the monsoon. We discuss the daily precipitation further in section 3.

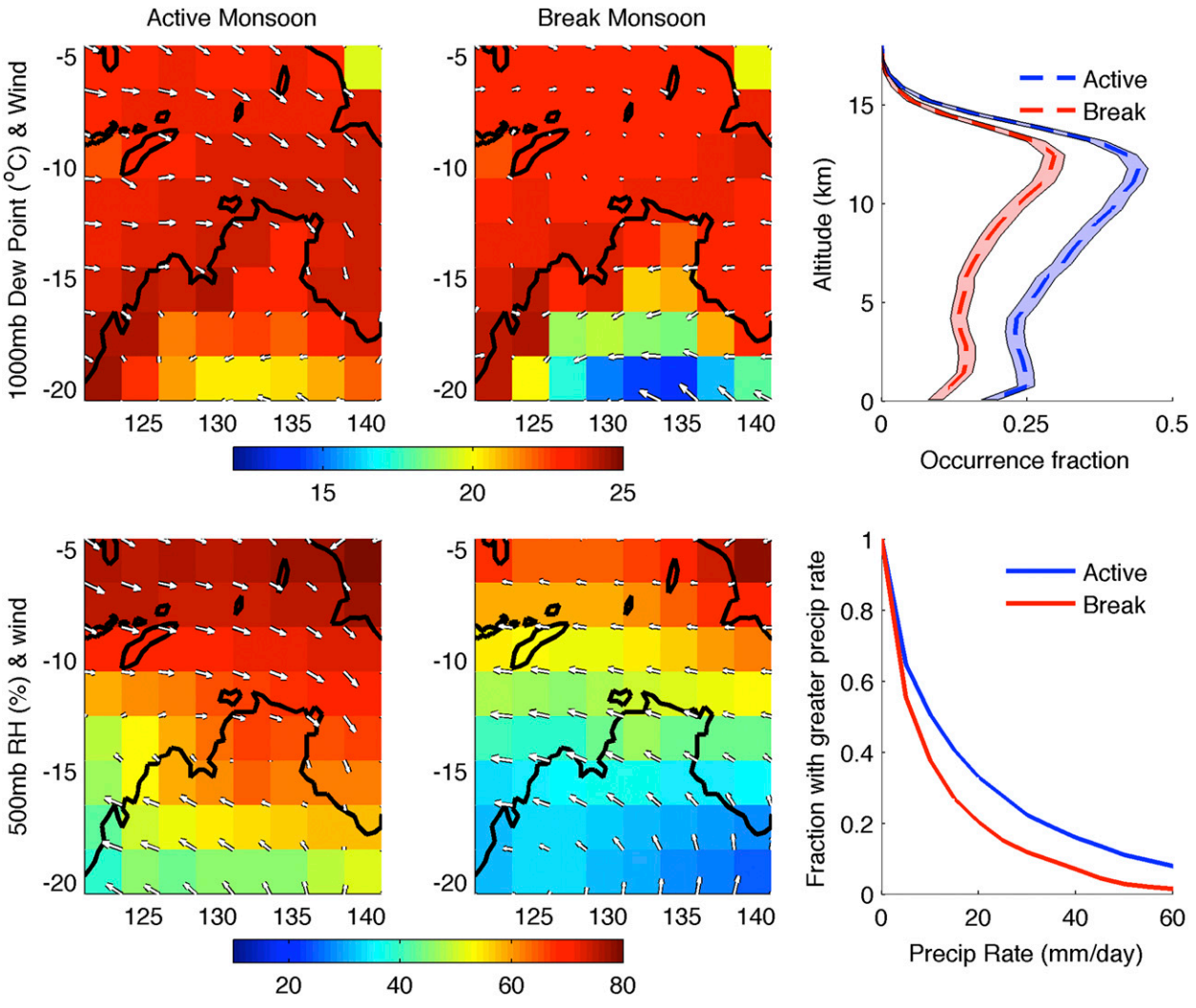

FIG. 1. (top) The 1000-hPa dewpoint and winds and (bottom) the 500-hPa relative humidity and winds as a function of latitude and longitude for (left) state 7, the active monsoon, and (center) state 8, the break monsoon. Maximum wind vector length corresponds to $8\,\mathrm{m\,s^{-1}}$. (right) Vertical profiles of (top) cloud occurrence and (bottom) distributions of daily precipitation rate for the two monsoon states. Cloud occurrence is defined as the fraction of time a radar echo of at least $-40\,\mathrm{dB}Z$ is detected by the vertically pointed millimeter cloud radar at the ARM site at Darwin. Shaded regions are 95% confidence limits, as estimated by a bootstrap algorithm. Precipitation distributions are only for days with rain, which is 78% of active days and 56% of break days.

3. Interannual variability

Our atmospheric classification technique provides rather different monsoon definitions than those used in previous studies and is not specifically tailored to identifying monsoon activity. Rather, as described in the previous section, it is based on a set of objective tests (stability and distinctiveness of radar profiles) and was originally designed and applied at midlatitudes. The technique includes no expert knowledge on the meteorology of Darwin and was not, for example, specifically guided toward identifying active and break periods of the monsoon. We therefore consider it important to verify that we are properly identifying periods of monsoon activity before using the classification to analyze research questions in sections 4 and 5. Our intent is not to show that this approach is superior to other approaches for the identification of monsoon onset; rather, the purpose of this section is to demonstrate that our method produces results consistent with previous studies by showing that it recreates some of the best-known features of Australian monsoon variability. We begin with the date of monsoon onset, perhaps the most studied feature of the monsoon. In Fig. 3 we show the time series of monsoon onset and retreat as defined by this study as well as those from two studies that

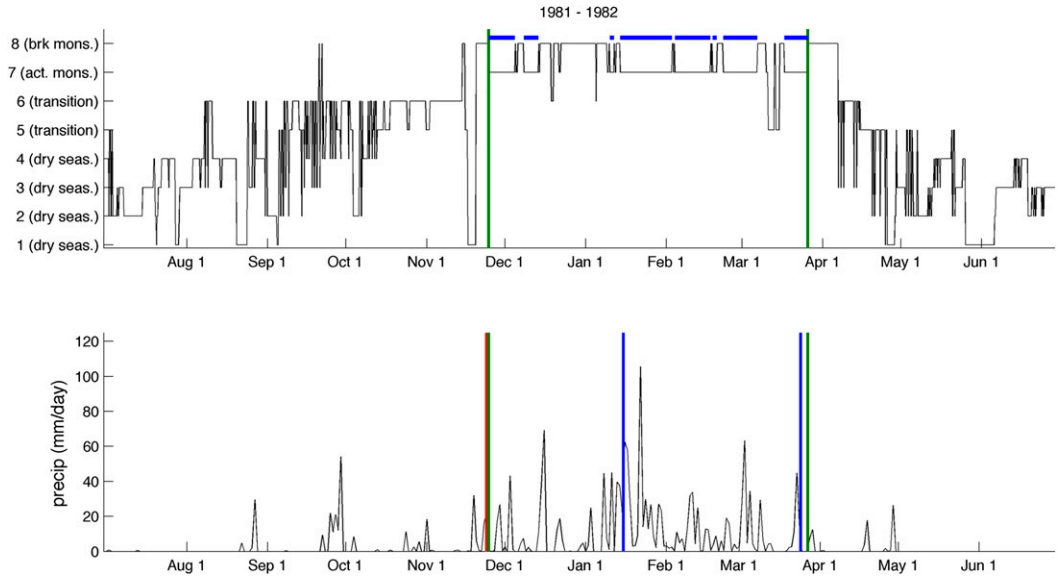

FIG. 2. Time series of (top) atmospheric state and (bottom) daily precipitation for the 1981/82 monsoon season. In (top), monsoon onset and retreat (vertical green lines) and active periods (horizontal blue bars) as defined in section 2 are shown. In (bottom), the onset and retreat as defined by this paper (vertical blue lines), Hendon and Liebmann (1990) (vertical red line), and Drosdowsky (1996) (vertical blue lines) are shown.

published tables of dates: Drosdowsky (1996) and Hendon and Liebmann (1990). Drosdowsky defines onset as the first period of at least 2 days when the vertically averaged 1000–500-hPa zonal wind exceeds a minimum westerly threshold while being overlaid by easterlies winds from 300 to 100 hPa. Hendon and Liebmann's definition of onset is the first simultaneous occurrence of westerly 850-hPa winds in the temporally smoothed times series at Darwin and average rainfall of 7.5 mm day^{-1} at several northern Australian weather stations. We also show the austral spring (September–November) average Southern Oscillation index (SOI) as provided by the Australian Bureau of Meteorology. As noted in the introduction, the date of monsoon onset has a well-established negative correlation with the Southern Oscillation in the preceding austral spring: that is, the monsoon starts earlier in La Niña years and later in El Niño years, while no such relationship has been found for the monsoon retreat. Our classification captures the same relationship between the Southern Oscillation and monsoon onset date as the previous studies and actually has a stronger relationship [$r = -0.49$ for our definition and $r = -0.38$ and -0.29 for Hendon and Liebmann (1990) and Drosdowsky (1996), respectively], although this may simply be as a result of covering different time periods. In overlapping years of study, our onset dates correlate with those of Drosdowsky with $r = 0.54$ and of Hendon and Liebmann with $r = 0.71$, while the two correlate with each other with $r = 0.61$. Kajikawa et al. (2010) also report similar magnitude correlations for their onset date ($r = 0.54$ with Drosdowsky, and $r = 0.59$ with Hendon and Liebmann).

Figure 3 also shows that our onset dates are earlier than those of the other studies. The mean onset date is 28–29 December for Drosdowsky (1996) and 24 December for Hendon and Liebmann (1990); it is 13 December by our definition. Other published mean onset dates include 24 (Holland 1986) and 16 December (Kajikawa et al. 2010). We think that this shift of up to two weeks, relative to the other definitions, is caused in

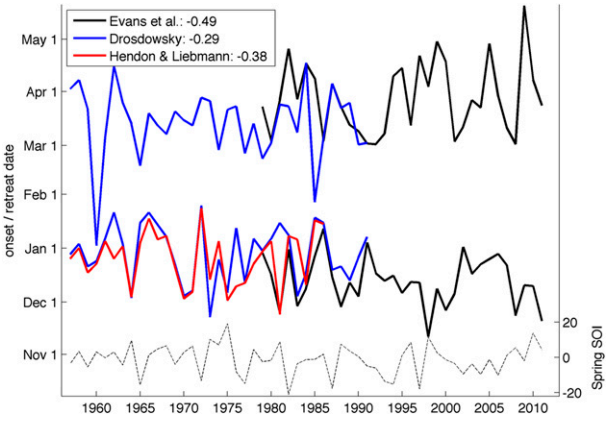

FIG. 3. Time series of monsoon onset (lower set of solid lines) and retreat (upper set of solid lines) according to this study (black), Drosdowsky (1996) (blue), and Hendon and Liebmann (1990) (red). The dashed black line shows the average September–November SOI. The year listed on the horizontal axis is the starting year of the monsoon season (i.e., 1960 is the 1960/61 season).

part by how we classify each ERA-Interim snapshot, and partly due to analyzing different time periods. Regarding our classification technique, while other studies establish a threshold and require some observed environmental conditions to exceed it, our definition requires that the large-scale pattern more closely resemble the active monsoon than the transitional or break monsoon patterns. We discuss this aspect of the classification further at the end of section 4. For similar reasons, our definition makes our mean retreat date (28 March) later than others (13 March for Drosdowsky). The limited number of overlapping years used in our study and used in Drosdowsky (1996) and Hendon and Liebmann (1990) may also contribute to the differences in start date, as we cannot determine from the available data whether decadal variability or very long-term trends might exist. We note that our mean onset date closely agrees with that of Kajikawa et al. (2010), which is the only one of the studies that calculates onset dates more recent than the 1991/92 season. Visual inspection of the results in Kajikawa, et al. shows that their onset dates for recent decades are earlier in the season than their onset dates from the early part of their dataset (the 1950s–60s). This suggests there may in fact be a long-term trend or variability at work that would contribute to our onset dates being earlier than those of previous studies.

We further investigate the differences between our dates and those of other studies by analyzing the daily precipitation recorded at Darwin International Airport. Returning to Fig. 2, we see an early period of precipitation in late November and early December. Both our study and Hendon and Liebmann (1990) find this active period to be the start of the monsoon, while the definition from Drosdowsky (1996) identifies the monsoon onset to be associated with a period of precipitation in mid-January. At the time of our onset, the cumulative precipitation for the water year (from June to June) is 17% of the total precipitation that fell in the 1981/82 year. At the time of Drosdowsky's onset 48% of the year's precipitation had already fallen, indicating that a substantial portion of the monsoon season had already occurred. We chose to show the 1981/82 season in Fig. 2 both because it has large disagreement for the onset date and because it is representative of how the disagreement occurs. Inspection of the other cases of large disagreement (1980/81 onset, 1982/83 retreat, 1983/84 onset, and 1985/86 onset and retreat) shows that for onsets the disagreeing study has not included an early period of precipitation and instead has assigned monsoon onset to the subsequent period of activity, while for retreats it is a late period of precipitation not included by the disagreeing study. In doing so, these two definitions for the monsoon sometimes do not include a substantial portion of the year's precipitation within the monsoon season. In the extreme case, only 16% of the precipitation in the 1985/86 season falls during the Drosdowsky-defined monsoon. Table 1 summarizes the differences in cumulative precipitation at the time of onset and retreat for each study. It shows that, by more regularly detecting these early and late periods of activity, this study has a more consistent fraction of the yearly precipitation falling at the time of monsoon onset and retreat, despite precipitation not being a part of our definitions. We take this as evidence that we are very reliably identifying the beginning and end of each monsoon season.

TABLE 1. Cumulative precipitation, as a percentage of the total precipitation from June to June that has occurred at the time of monsoon onset and retreat, according to various definitions. Onset and retreat refer to dates defined by this study, except for dates from Drosdowsky (1996) and Hendon and Liebmann (1990) denoted by D96 and H90, respectively. The mean value and standard deviation is given for each definition.

	Onset	D96 onset	H90 onset	Retreat	D96 retreat
Mean	16	30	26	92	85
Std dev	6	12	10	8	14

A second well-studied characteristic of the monsoon is the interannual variability of its seasonal intensity. As described in the introduction, La Niña conditions are correlated with more intense monsoon seasons by a number of metrics (Kajikawa et al. 2010; Drosdowsky 1996; McBride and Nicholls 1983). We find that the total number of days classified as active is significantly correlated with austral spring SOI ($p < 0.05$), as is the fraction of the monsoon season classified as active, albeit at a weaker significance level ($p = 0.07$). This weaker significance level is likely due to this metric being a function of monsoon season duration, which is in turn a function of retreat date. The retreat date is uncorrelated with the SOI, thus introducing some variability into this metric. The number of active days and the active fraction of observations are correlated at $r = 0.53$, implying that it is not purely a trade-off between active and break periods but also a lengthening of the monsoon season that contributes to the strengthening of the monsoon season during La Niña years.

A practical question is how far in advance ENSO indices provide information regarding the onset and intensity of the coming monsoon season. Nicholls et al. (1982) found significant correlations between austral winter [June–August (JJA)] mean surface pressure at Darwin and a variety of onset dates based on different levels of cumulative precipitation. The onset dates of Nicholls et al. have a similar range as ours (late October–early January), and surface pressure at Darwin is strongly

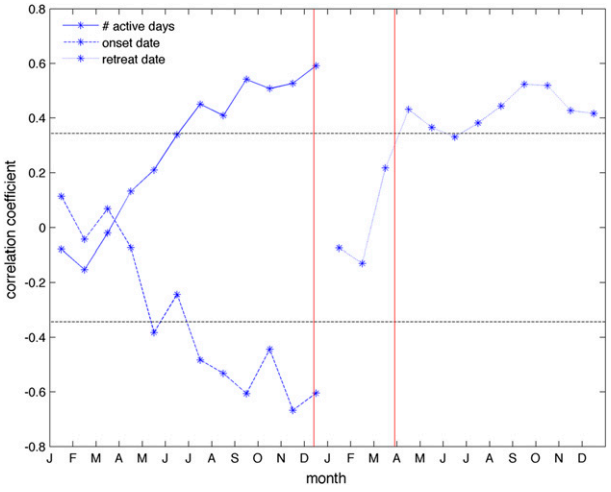

FIG. 4. Time evolution of the correlation coefficients between monthly average SOI and the number of active monsoon days (blue solid), onset date (blue dashed), and retreat date (blue dotted) for the years preceding and following the monsoon. Horizontal dashed black lines indicate 95% significance levels, estimated from the Fisher Z transformation. Vertical red lines indicate mean onset and retreat dates.

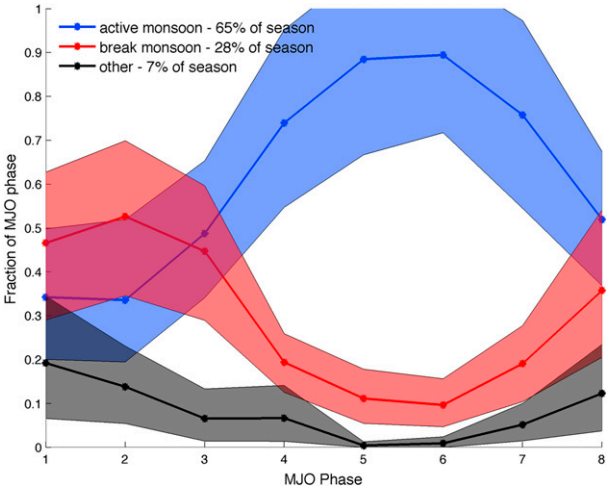

FIG. 5. The relative occurrence of different states for each MJO phase during the monsoon season. Monsoon season is defined as onset to retreat. Shaded regions indicate 95% confidence limits as estimated by a bootstrap algorithm operating on 33 yr of data. The overall fraction of the monsoon season occupied by each state/category is shown in the legend.

correlated with the SOI, so we would expect to see similar predictability using our methods. To determine how far back we have predictive skill, we calculate correlation coefficients for onset date and number of active days with monthly average SOI (Fig. 4). We find that, as early as the preceding July, the SOI index is significantly correlated with both onset date and the number of active days. While statistically significant, these correlations are rather weak for July at $r = 0.48$ and 0.45 for onset date and active days, respectively. The correlation with the SOI gradually grows stronger as monsoon season approaches, eventually reaching $r = 0.67$ and 0.53 for onset date and active days in November. This suggests that, while some degree of seasonal predictability is connected with ENSO, there are other important sources of variability, such as the timing of MJO events and midlatitude troughs, as well as the land–sea thermal contrast (Hung and Yanai 2004).

4. Intraseasonal variability

Within a single season, the monsoon goes through active and inactive periods on the scale of days to weeks. On these time scales, the MJO is a major driver of tropical variability. We investigate the role of the MJO using the Wheeler and Hendon (2004) definition of MJO phase. This definition is such that, as the MJO propagates eastward from the Indian Ocean out into the Pacific, the phase number steadily increases to represent the geographic location of enhanced convection. Darwin experiences enhanced convection during phases 4–6 and suppressed convection during phases 8, 1, and 2. In our analysis, we omit periods of weak MJO activity, as defined by when the Wheeler and Hendon index has amplitude less than one. This excludes 36% of the monsoon periods but has a negligible effect on the statistics described below, as the distribution of atmospheric states during weak MJO activity closely follows that of strong MJO periods. Wheeler et al. (2009) demonstrate that the phase of the MJO according to these definitions has significant relationships with summertime precipitation in northern Australia, suggesting that the phase definition should be suitable for investigating the timing of active periods of the monsoon.

Figure 5 shows the distribution of atmospheric states during the monsoon season for each phase of the MJO. Monsoon season here is defined as the period from onset until retreat, as defined in section 2. Overall, 65% of the observations from the 33 monsoon seasons are classified as active, while 28% are classified as break periods. When the MJO is in a position to enhance convection at Darwin, the monsoon is much more likely to be active, reaching probabilities of nearly 90% during phases 5 and 6. Similarly, when the MJO is in a location associated with suppressed convection at Darwin, break periods become more likely and are a majority of the observations during phases 1 and 2. For both the active and break periods, the largest changes in probability of occurrence happen at the transition from phase 3 to 4 and from phase 7 to 8. This suggests that active periods are initiating with the arrival of the MJO and break periods with the departure.

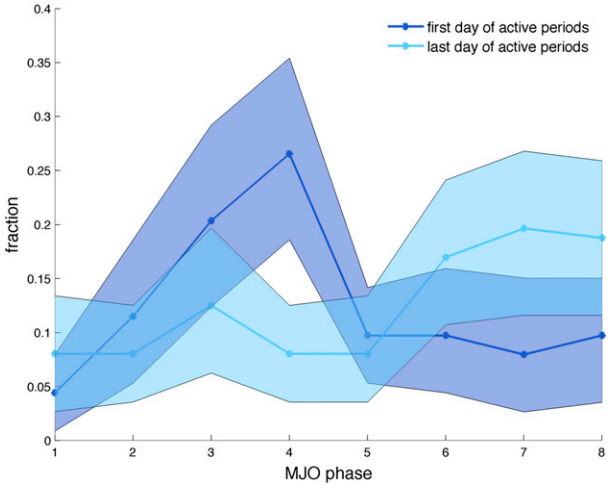

FIG. 6. Distribution of MJO phase for the first day of 179 active periods (dark blue) and the last day of each active period (light blue). Shading represents 95% confidence limits, as calculated by a bootstrap algorithm.

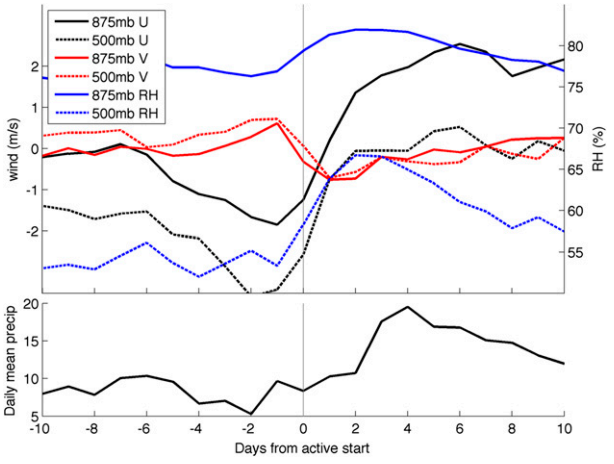

FIG. 7. (top) Domain mean values of zonal (black) and meridional (red) wind (left axis values), and relative humidity (blue; right axis values) at 875 (solid lines) and 500 mb (dashed lines). (bottom) Mean daily precipitation at Darwin International Airport. Values are composited relative to the first day of each active period.

To investigate this further, we compute the distribution of MJO phase for the first day of each active period and the last day of each active period (Fig. 6). We define an active period as at least four consecutive observations (24 h) being classified as the active monsoon (state 7). We see that active periods most frequently begin during MJO phases 3 and 4, earlier than the peak of overall active occurrence, phases 5 and 6. This implies that, by the time the MJO reaches phases 5 and 6, most active periods have already begun. Similarly, the active monsoon periods end most often during phases 7 and 8, which is earlier in the MJO cycle than the peak of break monsoon occurrence. This again suggests that, by the time the MJO reaches phases 1 and 2, most of the active periods have already ended. We conclude that the MJO plays a strong role in both initiating and terminating the active periods of the monsoon.

That the plurality of active periods begin during phase 4 is not surprising, as this is the first phase with enhanced convection at Darwin (Wheeler and Hendon, 2004). By the time the MJO reaches phase 4, the wind anomalies become westerly and cyclonic, making the snapshots very much like our definition of the active monsoon and readily initiating an active period. It is interesting, however, that the second-most active periods begin during MJO phase 3, before the enhanced convection reaches Darwin. Composites by MJO phase for our region of classification confirm that the westerly wind anomaly has, on average, not yet reached the region during phase 3, so one might reasonably ask what prompts the classifier to identify these observations as the start of active periods. Compositing relative humidity for each MJO phase shows a moisture anomaly at both low and middle levels that leads the change in winds, consistent with observations of MJO related anomalies (Benedict and Randall 2007). By phase 3 of the MJO, this moisture anomaly has changed from the deeply negative values of phases 1 and 2 to near-neutral values, making the moisture profile of phase 3 more similar to the active monsoon than to any other atmospheric state. Similarly, we see a dry anomaly which precedes the change in winds helping to end the active periods during phases 6 and 7.

Still, the zonal wind is as important to the classification as relative humidity, making it somewhat puzzling that a moisture anomaly could, on its own, initiate an active period. To explore this, we composite the phase 3 snapshots that are the first day of an active period and find that these snapshots are both more humid and more westerly than the overall average phase 3 values. This is to say that it is the phase 3 snapshots that begin active periods are ones with the convective anomaly further east than average. The variability in atmospheric conditions that exists for a single MJO phase is enough to allow active periods of the monsoon to begin in phase 3, even if the phase, on average, does not enhance convection. We confirm that active periods are being triggered by changes in both wind and humidity by compositing the horizontal winds, relative humidity, and daily precipitation at Darwin for 10 days before and after the initiation of each active period (Fig. 7). As can be seen, the zonal wind, meridional wind, and relative humidity are all rapidly changing at the start of active periods. These changes begin the day before the active period begins, grow strong enough to initiate the active period, and continue to grow for the next 1–3 days. The

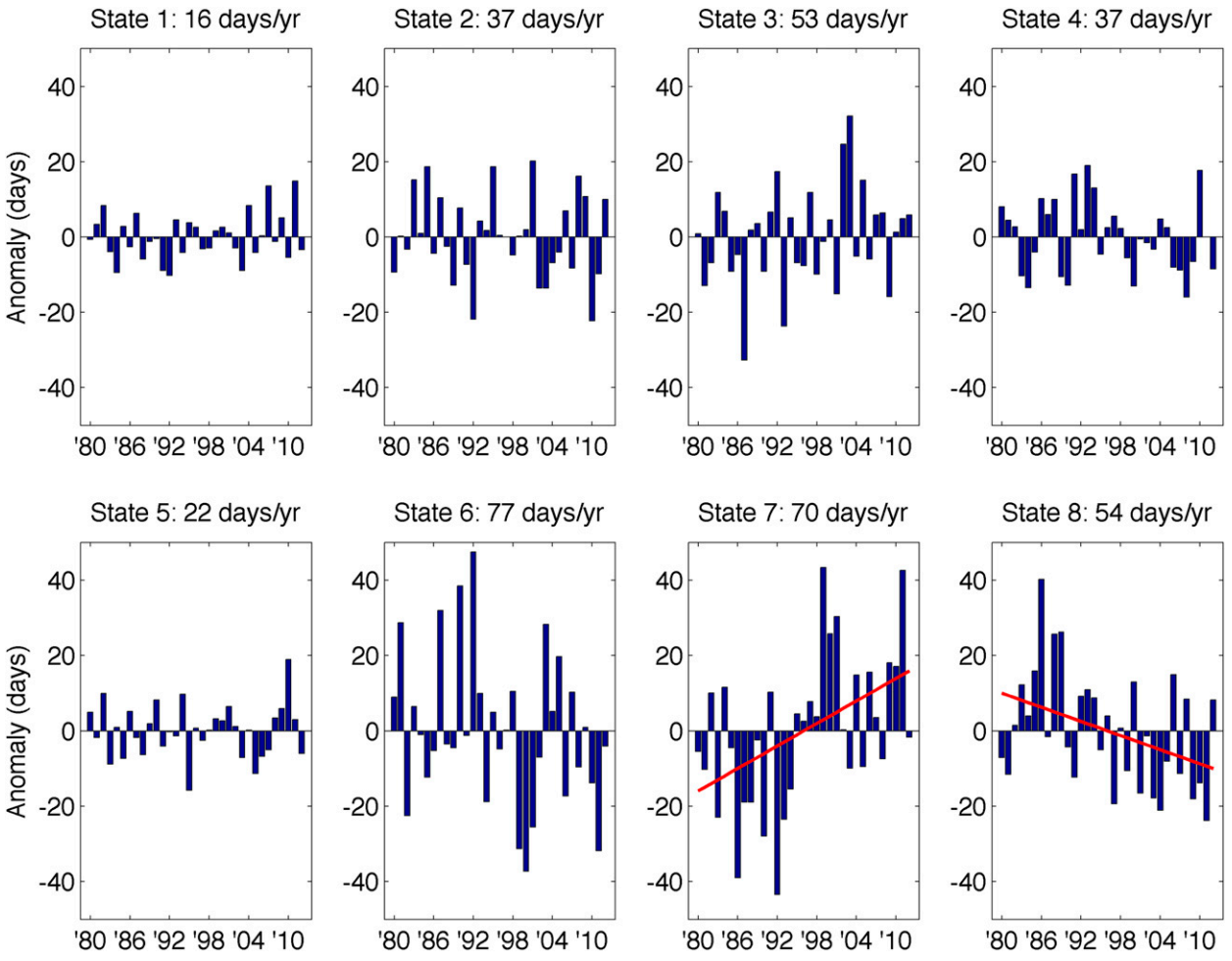

FIG. 8. Frequency of occurrence of atmospheric states over the ERA-Interim period, calculated as the anomaly, in days, from the mean. Years are calculated from the midpoint of one calendar year to the midpoint of the next. Labeled years are the first calendar year of each year period: for example, 1983 indicates the 1983/84 period. Red lines indicate states with statistically significant trends. The mean number of occurrences of each state is shown in the panel titles.

daily precipitation reaches its minimum 2 days before the event begins and rises steadily for several days before peaking at 3 and 4 days after the active period begins. This is in keeping with the idea that the active period begins as the MJO approaches, strengthens as the convective anomaly reaches Darwin, and then ends as the anomaly departs. Collectively, we take this as evidence that the active periods identified are not simply the result of an anomaly in a single variable but rather are the coherent establishment of a monsoon circulation and that we are identifying them from their beginning, rather than their peak.

5. Trends

The length of our 33-yr period of study allows us to investigate trends in the monsoon metrics. While we find trends of earlier onset, later retreat, and greater duration, none of these trends is significant at the 95% confidence limit. We do, however, find a significant positive trend in the number of days classified as the active monsoon and a significant negative trend in the number of days classified as the break monsoon (Fig. 8). The trend is approximately 10 days per decade for the active monsoon and −6 days per decade for the break monsoon. The discrepancy between these values is accounted for by a small change in the number of days that the classifier identifies as transition season states rather than monsoon states. The change in the number of transition season days is not significant at the 95% confidence level. The increase in active monsoon days at the expense of break monsoon and transition days suggests that the monsoon has become both longer and more active in recent decades. This is consistent with the observed trend in SOI. However, when we tested the relationship between the number of active days and the

SOI in section 3, we found that the number of active days increases by approximately 1.2 for each unit of the SOI index and the trend in the SOI index during the period of study is 3.4 units per decade. Multiplying the two together suggests that the trend in the SOI during the period of study is only responsible for approximately 4 extra active days per decade, or 40% of the trend in the number of active days. Of course this simple calculation assumes a linear relationship between the SOI and the number of active days is a good model for this relationship. Nonetheless, while a fraction of the increase in precipitation at Darwin is related to ENSO, it is apparent that factors other than ENSO are also important.

To further investigate the idea of an intensifying monsoon, we turn to daily precipitation observations at Darwin International Airport. We use these data because so far as we know they are the only high-quality observations of precipitation that span the full ERA-Interim period, which starts in 1979. These data are available through the Australian Bureau of Meteorology and extend back to 1941. We composite these data according to state and year by assigning each classification time the daily averaged precipitation from the day on which it occurred. Again, our year periods begin and end in June. This preserves a continuous monsoon period and guarantees that the premonsoon and postmonsoon transition seasons are counted in the same year as the monsoon. We consider it important to include the transition seasons in the same water year as the monsoon in order to account for the effect of the apparent trade-off in days classified as the active monsoon and days classified as transition periods. The dry seasons at Darwin are divided in our water years from June to June, but their contribution is negligibly small with regard to total annual rainfall.

Annual rainfall at Darwin International Airport has increased by 6.5 mm yr^{-1} ($p = 0.004$) since the start of the record in 1941, as shown in Fig. 9. During the period of the E12 classification (1979–2012), the trend has increased to 9.5 mm yr^{-1}, though it is no longer significant over this shorter period ($p = 0.23$). Nonetheless, as the more recent period represents nearly half of a longer, highly statistically significant trend, and as the recent trend is notably large, it is interesting to explore why Darwin has received more rain in recent years. The precipitation measured at a single station represents only a very small area, which inherently leads to a large annual variability. However, analyzing data over many years significantly reduces the impact of variability due to spatial sampling. The change in total rainfall can be caused by either a change in the frequency of occurrence of the atmospheric states (rainy states becoming more frequent) or by a change in the precipitation associated

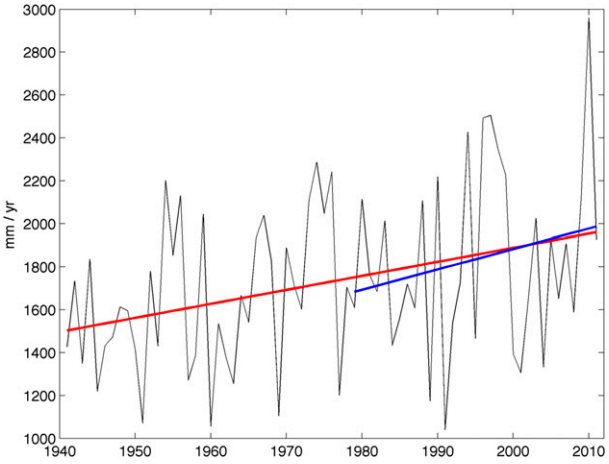

FIG. 9. Annual rainfall at Darwin International Airport. Years are calculated from the midpoint of one calendar year to the midpoint of the next (i.e., from June to June). Labeled years are the first calendar year of each year period: for example, 1980 indicates the 1980/81 period. The trend over the full period (6.5 mm yr^{-1}; $p = 0.004$) is shown in red, while the trend over the period of this study (9.5 mm yr^{-1}; $p = 0.23$) is shown in blue.

with each state (states becoming rainier). Among the individual atmospheric states, only state 3 has a trend, in this case a negative one, in mean precipitation that is significant at 95% confidence. State 3 is a very dry state that rains very rarely and then only weakly, so a trend in its precipitation is not important to the overall trend. Following the method of Catto et al. (2012a, hereafter C12), we decompose the overall precipitation trend into the contributions from changes in frequency of occurrence and contributions from changes in mean precipitation. Mathematically, this can be described as follows:

$$\Delta R = \sum_i N_i \Delta P_i + \sum_i \Delta N_i P_i + \sum_i \Delta N_i \Delta P_i, \qquad (1)$$

where ΔR is the total rainfall trend (mm yr^{-1}), N is the annual mean number of occurrences of state i, P is the mean precipitation for the state i, and ΔN and ΔP are the linear trends in those values for each state.

Figure 10 shows the contributions to the overall trend from both changes in the mean precipitation of each atmospheric states [the first term of Eq. (1)] and changes in their frequency of occurrence (the second term). We omit the third term of Eq. (1) because the second-order contributions are much smaller than the other terms. The decomposition demonstrates that the observed increase in annual precipitation at Darwin is almost entirely due to the increase in the number of active monsoon days since 1979. This increase in the frequency of occurrence of the rainiest state of the classification more than makes up for the reduction in both the

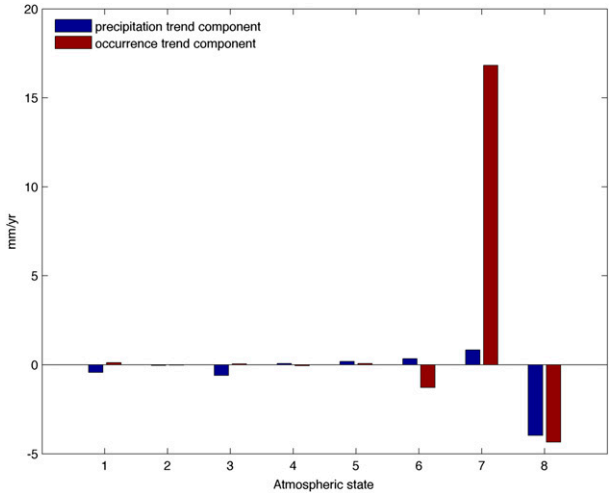

FIG. 10. Contributions to the 33-yr trend in annual rainfall at Darwin International Airport. Blue bars are the contribution due to trends in within-state mean precipitation and red bars are the contribution due to trends in the frequency of occurrence of the states.

occurrence and mean precipitation of state 8. This is broadly in keeping with the findings of C12, who find that the increase in wet season precipitation at Darwin is due to an increase in the occurrence of rainy regimes at the expense of fewer occurrences of dry regimes. However, the regimes used in C12 and the states we use do not perfectly match up. In section 6 we compare the two classifications and discuss insights these difference yield into the causes of the precipitation trend at Darwin.

Interestingly, while the annual frequency of occurrence of the active monsoon dominates the 33-yr trend in precipitation at Darwin, the interannual variability of total annual precipitation is better explained by interannual changes in the mean daily precipitation of each state. The percent of the variance in annual precipitation (r^2) over the 33-yr record due to both the annual occurrence of each state and the annual mean precipitation of each state is provided in Table 2. Variations in the active monsoon state explain by far the largest amount of variability in total annual precipitation, in terms of both frequency of occurrence (38%) and mean precipitation (47%), with variations in mean precipitation being somewhat more important. Because the frequency of occurrence of one state is strongly correlated with the frequency of occurrence of other states during each season (dry, transition, and monsoon), we also include three combinations of states. The collective total of states 1–4 is the dry season, states 5 and 6 are the transition season, and states 7 and 8 are the monsoon season. As expected, variations in mean daily precipitation during the monsoon season explain the majority of the variance in total rainfall (r^2 of 75%). However, changes in annual mean daily precipitation may well be partly due to the spatial heterogeneity of precipitation, given the high spatial variability of precipitation measurements. It is unclear how much of the within-state variability is simply a result of spatial variability (which will tend to average out in the longer-term trend analysis) rather than true dynamically driven variability.

6. Discussion and conclusions

Our analysis uses an atmospheric classification for northern Australia to objectively identify dates of monsoon onset and retreat, periods during which the monsoon is active, and seasonal measures of monsoon intensity. We use these data to demonstrate that our method is capable of reproducing previously identified relationships between ENSO and monsoon onset and seasonal intensity. This, along with consistently capturing most of the cumulative precipitation with in our monsoon periods, gives us confidence that our method is accurately identifying periods of monsoon activity. We then use our classification-based metrics to show that active periods of the monsoon begin as the MJO approaches the region and end as the MJO leaves the region. Finally, we use this classification to calculate the contributions to the observed precipitation trend at Darwin International Airport from changes in large-scale circulation patterns (state occurrence) and changes in local-scale thermodynamics (mean precipitation within each state) and find that the positive trend in precipitation is entirely due to an increase in the number of active monsoon days (large-scale circulation patterns)

TABLE 2. Percent of the variance in annual precipitation (r^2) at Darwin over the 33-yr record that is explained by 1) the annual occurrence of each state (AnnO), measured in days, and 2) the annual mean precipitation associated with each state (AvgP). The last three columns are combined values of r^2: that is, the combined annual occurrence and weighted mean precipitation for multiple states. Dry refers to the sum occurrence of states 1–4 and their combined mean precipitation, transition refers to the sum of states 5 and 6, and monsoon refers to the sum of states 7 and 8.

	State 1	State 2	State 3	State 4	State 5	State 6	State 7	State 8	Dry	Transition	Monsoon
AnnO	6	0	0	0	0	18	38	8	0	21	21
AvgP	1	0	2	1	10	1	47	9	3	16	75

with no significant change in the mean daily precipitation during the active monsoon.

The fact that the Australian monsoon is influenced by ENSO is well established, but an interesting related question is whether the inverse is true: that is, does the monsoon affect ENSO? Holland (1986) found that the onset date was negatively correlated with equatorial Pacific SSTs nine months later: that is, an early monsoon was more likely to be followed by El Niño conditions the following austral spring. Drosdowsky (1996) tested this but could not identify such a relationship. Using our definition of onset, we do not find any relationship between onset date and either the SOI or the Niño-3.4 index at any time after the retreat of the monsoon. We do, however, find a significant positive correlation between the retreat date and the following winter/spring SOI: that is, a later retreat is more likely to be followed by La Niña conditions (Fig. 4). Determining the cause of this correlation is beyond the scope of this study, but we offer one possible mechanism. A stronger Walker circulation associated with increased deep convection over the Maritime Continent would be associated with stronger easterlies over the west Pacific, which would act to support La Niña conditions.

Our finding that the passage of the MJO initiates active and break periods of the monsoon may help us understand the difference in findings between Holland (1986) and Drosdowsky (1996). As in the Drosdowsky study, and in contrast to that of Holland, when we calculate the period from one active period to the next we find a broad, flat distribution with no preferred time scale. This can be reconciled with our findings from section 4 by recalling that there is a large range in the lifetime of an MJO event as it crosses the Indian and Pacific Oceans. For example, Kim et al. (2014) found that MJO events with a strong dry anomaly leading the enhanced convection last, on average, 40% longer than those that do not. Such a range of MJO lifetimes makes an analysis of the return time or duration of active periods less likely to show the influence of the MJO. That we were able to find a clear influence of the MJO (Figs. 5 and 6) shows the value of analyzing the role of the MJO using an index like that of Wheeler and Hendon (2004), which allows for the discovery of MJO-induced effects that do not have a clear 40–50-day period.

The trend toward greater occurrence of the active monsoon is a topic that merits further study. The trend in ENSO does not appear to be responsible for the total trend in the number of active days. We cannot determine from the available data if the trend in active days is due to decadal variability or the result of anthropogenic forcing. It is possible that this question can be addressed with the use of general circulation models (GCMs). For example, Rotstayn et al. (2007) found that including anthropogenic aerosols in runs of the Commonwealth Scientific and Industrial Research Organisation (CSIRO) GCM created circulation and precipitation changes over northern Australia that helped to explain the observed trends. The model in question has been shown to have an inaccurate relationship between ENSO and precipitation in northwest Australia (Shi et al. 2008), but the possibility of an aerosol–precipitation relationship is worth investigating in other GCMs. GCM projections of precipitation over northern Australia for the twenty-first century disagree whether precipitation will increase or decrease. This difference can be understood in part by changes to the frequency of dynamic regimes and the precipitation associated with them (Moise et al. 2012). If GCM output was classified according to the atmospheric states presented here, it would be straightforward to carry out the type of analysis performed here and assess whether different GCM runs reproduce the observed changes in the number of active days over the past few decades and whether that trend continues into the future.

Our determination that the contributions to the recent precipitation trend at Darwin are dominated primarily by changes in the frequency of occurrence of the deep monsoon state (state 7 in Fig. 10) provides evidence that the precipitation distributions associated with the atmospheric states are stable in time. The precipitation distribution associated with the active monsoon (state 7) remains constant, but the occurrence of the active monsoon increases in time. Unfortunately, the trend contribution from the break monsoon state (state 8) is composed of equal parts of a change in frequency of occurrence and a change in mean precipitation. We are not entirely sure of the explanation for this. A likely possibility is that the break monsoon state is really composed of two states with somewhat different precipitation distributions. Subdividing it into two states might then identify changes in the relative occurrence frequency of those two states as driving the precipitation trend. There is also the possibility that we are not clearly separating the two transition states from the monsoon break state and this is affecting our results because the precipitation rate distribution from the break monsoon has higher rain rates than that from the transition states. In applying our technique to the ARM Southern Great Plains site, which has a much longer cloud-radar data record, we have found that the longer data record leads, not surprisingly, to the identification of more states and a greater discrimination among the states. We expect that using a longer cloud-radar data record at Darwin than was used in generating our current eight states

described in E12 will enable us to further refine the classification and perhaps resolve this issue.

Comparison to the classification of C12 produces some interesting results that lead to further research questions. C12 conclude that the trend in precipitation is due to changes in the frequency of occurrence of regimes, which is broadly in agreement with our conclusion; however, the particular states/regimes involved in the two classification schemes do not match up cleanly. C12 uses the classification described by Pope et al. (2009) to decompose the observed precipitation trend. In Evans et al. (2012), we compare our classification to that of Pope et al. and conclude that their deep west regime is similar to our state 7, and that their moist east regime is similar to our state 8. Directly comparing our time series of atmospheric state to the time series of regime used in C12 provides a more nuanced understanding of the comparison between the two classifications. We find that approximately 60% of the days in the deep west regime fall within our state 7 (active monsoon), with 30% and 10% being classified as state 8 (break monsoon) and state 6 (premonsoon transition), respectively. Our state 7 comprises a much larger fraction of the monsoon season than the deep west regime and also contains significant amounts of the Pope et al. (2009) shallow west and moist east regimes. We conclude that our state 7 is a broader definition of the active monsoon than the deep west regime. The Pope et al. (2009) moist east regime, meanwhile, is a much larger fraction of the monsoon season than our state 8 and contains large fractions of our state 6 (which is drier) and state 7 (which is much wetter). This leads us to believe that our state 8 is a more restrictive definition of a break period of the monsoon.

As described in section 5, we find a statistically significant increase in the frequency of occurrence of the active monsoon at the cost of the break monsoon and transition states. C12, however, find only a weakly positive trend that is not statistically significant in the frequency of the deep west regime. Taken together, this suggests that it is the non–deep west components of state 7: that is, the moderately active periods that have become more frequent. C12 find a positive trend in the occurrence of their moist east regime, while we find a negative trend in the occurrence of our state 8. This suggests that it is the more active elements of the Pope et al. (2009) moist east regime that are responsible for their positive trend, while it is the least active elements of state 8 that are responsible for that state's negative trend in our result. This supports the conclusion that periods of moderate active monsoon have been increasing in frequency at the expense of the weakest periods of the monsoon. We think this conclusion is interesting and warrants further investigation through a more detailed comparison of the results of the two different classification techniques.

Acknowledgments. We thank Dr. Jennifer Catto for generously providing the time series of regimes used in her study. We thank the Australian Bureau of Meteorology's Climate Data Services group for providing daily rainfall observations from Darwin International Airport and monthly mean SOI data on their website. We also thank The Centre for Australian Weather and Climate Research for providing the Wheeler and Hendon MJO indices online. This research was supported by the U.S. Department of Energy Atmospheric System Research program under Contract DESC0002472.

REFERENCES

Benedict, J. J., and D. A. Randall, 2007: Observed characteristics of the MJO relative to maximum rainfall. *J. Atmos. Sci.,* **64,** 2332–2354, doi:10.1175/JAS3968.1.

Catto, J. L., C. Jakob, and N. Nicholls, 2012a: The influence of changes in synoptic regimes on north Australian wet season rainfall trends. *J. Geophys. Res.,* **117,** D10102, doi:10.1029/2012JD017472.

——, N. Nicholls, and C. Jakob, 2012b: North Australian sea surface temperatures and El Nino–Southern Oscillation in observations and models. *J. Climate,* **25,** 5011–5029, doi:10.1175/JCLI-D-11-00311.1.

Drosdowsky, W., 1996: Variability of the Australian summer monsoon at Darwin: 1957–1992. *J. Climate,* **9,** 85–96, doi:10.1175/1520-0442(1996)009<0085:VOTASM>2.0.CO;2.

Evans, S. M., R. T. Marchand, T. P. Ackerman, and N. Beagley, 2012: Identification and analysis of atmospheric states and associated cloud properties for Darwin, Australia. *J. Geophys. Res.,* **117,** D06204, doi:10.1029/2011JD017010.

Hendon, H. H., and B. Liebmann, 1990: A composite study of the onset of the Australian summer monsoon. *J. Atmos. Sci.,* **47,** 2227–2240, doi:10.1175/1520-0469(1990)047<2227:ACSOOO>2.0.CO;2.

Hennessey, K. J., R. Suppiah, and C. M. Page, 1999: Australian rainfall changes, 1910-1995. *Aust. Meteor. Mag.,* **48,** 1–13.

Holland, G. J., 1986: Interannual variability of the Australian summer monsoon at Darwin: 1952–82. *Mon. Wea. Rev.,* **114,** 594–604, doi:10.1175/1520-0493(1986)114<0594:IVOTAS>2.0.CO;2.

Hung, C., and M. Yanai, 2004: Factors contributing to the onset of the Australian summer monsoon. *Quart. J. Roy. Meteor. Soc.,* **130,** 739–758, doi:10.1256/qj.02.191.

Kajikawa, Y., B. Wang, and J. Yang, 2010: A multi-time scale Australian monsoon index. *Int. J. Climatol.,* **30,** 1114–1120, doi:10.1002/joc.1955.

Kim, D., J.-S. Kug, and A. H. Sobel, 2014: Propagating versus nonpropagating Madden–Julian oscillation events. *J. Climate,* **27,** 111–125, doi:10.1175/JCLI-D-13-00084.1.

Madden, R. A., and P. R. Julian, 1972: Description of global-scale circulation cells in the tropics with a 40-50 day period. *J. Atmos. Sci.,* **29,** 1109–1123, doi:10.1175/1520-0469(1972)029<1109:DOGSCC>2.0.CO;2.

Marchand, R., N. Beagley, and T. Ackerman, 2009: Evaluation of hydrometeor occurrence profiles in the multiscale modeling framework climate model using atmospheric classification. *J. Climate,* **22,** 4557–4573, doi:10.1175/2009JCLI2638.1.

McBride, J. L., and N. Nicholls, 1983: Seasonal relationships between Australian rainfall and the Southern Oscillation. *Mon. Wea. Rev.,* **111,** 1998–2004, doi:10.1175/1520-0493(1983)111<1998:SRBARA>2.0.CO;2.

Moise, A. F., R. A. Colman, and J. R. Brown, 2012: Behind uncertainties in projections of Australian tropical climate: Analysis of 19 CMIP3 models. *J. Geophys. Res.,* **117,** D10103, doi:10.1029/2011JD017365.

Nicholls, N., J. L. McBride, and R. J. Ormerod, 1982: On predicting the onset of the Australian wet season at Darwin. *Mon. Wea. Rev.,* **110,** 14–17, doi:10.1175/1520-0493(1982)110<0014:OPTOOT>2.0.CO;2.

Pope, M., C. Jakob, and M. J. Reeder, 2009: Regimes of the north Australian wet season. *J. Climate,* **22,** 6699–6715, doi:10.1175/2009JCLI3057.1.

Rotstayn, L. D., and Coauthors, 2007: Have Australian rainfall and cloudiness increased due to the remote effects of Asian anthropogenic aerosols? *J. Geophys. Res.,* **112,** D09202, doi:10.1029/2006JD007712.

Shi, G., J. Ribbe, W. Cai, and T. Cowan 2008: An interpretation of Australia rainfall predictions. *Geophys. Res. Lett.,* **35,** L02702, doi:10.1029/2007GL032436.

Taschetto, A. S., and M. H. England, 2009: An analysis of of late twentieth century trends in Australian rainfall. *Int. J. Climatol.,* **29,** 791–807, doi:10.1002/joc.1736.

Wheeler, M. C., and H. H. Hendon, 2004: An all-season real-time multivariate MJO index: Development of an index for monitoring and prediction. *Mon. Wea. Rev.,* **132,** 1917–1932, doi:10.1175/1520-0493(2004)132<1917:AARMMI>2.0.CO;2.

——, ——, S. Cleland, H. Meinke, and A. Donald, 2009: Impacts of the Madden–Julian oscillation on Australian rainfall and circulation. *J. Climate,* **22,** 1482–1498, doi:10.1175/2008JCLI2595.1.

Zhang, C., 2005: Madden-Julian Oscillation. *Rev. Geophys.,* **43,** RG2003, doi:10.1029/2004RG000158.